ELSEVIER

Journal of Power Sources 72 (1998) 150–158

JOURNAL OF POWER SOURCES

Degradation mechanism of layered MnO_2 cathodes in $Zn/ZnSO_4/MnO_2$ rechargeable cells

Sa Heum Kim, Seung Mo Oh *

Department of Chemical Technology, College of Engineering, Seoul National University, Seoul 151-742, South Korea

Received 3 June 1997; revised 1 August 1997; accepted 30 August 1997

Abstract

Layered-type MnO_2 (δ- or naturally occurring birnessite-related MnO_2) electrodes that suffer capacity degradation during extended cycling in $Zn/ZnSO_4/MnO_2$ rechargeable cells are investigated. When the composite cathodes consisting of MnO_2 powder, carbon additive and Teflon binder are galvanostatically cycled in the potential range of 1.0–1.9 V (vs. Zn/Zn^{2+}) where a two-step, two-electron charge/discharge reaction occurs, the cathodes lose their capacities within a few cycles. Such an abrupt capacity loss is found to be caused partly by the formation of basic zinc sulfates (BZS, $ZnSO_4 \cdot 3Zn(OH)_2 \cdot nH_2O$) on the cathode surface, and also by the Mn losses due to the irreversible nature of the cathodic cell reaction: Mn^{2+} ions, once produced during the discharge step, are not fully restored to MnO_2 during the charging period. An addition of 0.1–0.5 M $MnSO_4$ to 2 M $ZnSO_4$ electrolyte, however, greatly alleviates these failure modes. With this addition, the Mn losses become insignificant as a result of facilitation in the charging reaction and BZS formation is discouraged. Carbon additives loaded in the composite MnO_2 cathodes also critically affect the cathode cyclabilities by controlling the rate of charging reaction: the cathodes loaded with acetylene blacks display superior cyclabilities to those containing furnace blacks. From one observation whereby the acetylene blacks possess a lesser amount of surface oxygenic species than the furnace blacks and the other whereby the charging reaction more readily occurs in the former cathodes, it is proposed that the charging (deposition) reaction is significantly hindered by the presence of surface oxygenic species on carbon additives. Electron micrographs of cycled MnO_2 cathodes reveal that larger and porous MnO_2 deposits are well-grown on the acetylene-black-loaded cathodes whereas only irregular-shaped smaller deposits are formed on the furnace-black-loaded cathodes.

Keywords: Rechargeable $Zn/ZnSO_4/MnO_2$ cells; Layered MnO_2; Acetylene black; Furnace black; Basic zinc sulfate (BZS)

1. Introduction

The Zn/MnO_2 system, with features such as good specific energy, good specific power, and the use of relatively cheap and low-polluting electrode materials, has traditionally provided one of the most popular primary cells [1,2]. These advantageous characteristics, combined with disposal problems encountered with primary cells, has prompted considerable efforts to develop their secondary counterparts. Until now, however, few successful products, except the RENEWAL alkaline batteries of Rayovac [3], have entered the market. It is known that this difficulty arises from the problems of zinc corrosion and the formation of electrochemically inactive products on the MnO_2 electrode surface [1,2]. Recently, aqueous $ZnSO_4$ solution has been exploited as a replacement for conventional alkaline electrolytes and has produced some promising results [4–6]. The literature indicates that, in aqueous $ZnSO_4$ electrolyte, the charge/discharge reactions on both the Zn anode and the MnO_2 cathode are reversible and the MnO_2 cathodes can be charged/discharged up to two-electron capacities.

Several MnO_2 phases have been tested as cathode materials for Zn/MnO_2 rechargeable cells. Among these, layered-type MnO_2 materials (δ-MnO_2 or naturally occurring birnessite-related MnO_2) are considered to be attractive since they, with a relatively wide interlayer gap, provide a favourable pathway for ionic diffusion during the charge/discharge reactions. Several reports on their preparation and cathodic performance in Zn/MnO_2 or Li/MnO_2 cells have already been documented [4,7–10].

* Corresponding author. Tel: +82-2-880-7074; fax: +82-2-888-1604; e-mail: seungoh@plaza.snu.ac.kr.

By contrast, details on the cathode failure mechanisms encountered in $Zn/ZnSO_4/MnO_2$ rechargeable cells have not been reported. The first half of this paper deals with this issue.

In the fabrication of composite electrodes for battery applications, carbons are added to improve electrode conductivity [1,2,11]. Here, carbons are mixed with active materials and binder to form a plate. The role of carbon additives is to provide an electron channel between the current-collector and the less-conductive active materials. On this basis, the physicochemical properties of carbon additives in terms of surface area, particle size, and intrinsic conductivity, as well as their loading and dispersion, are important variables since they determine electrode resistivity [11,12]. In the selection of carbon additives, however, the possibility of cell reactions and/or electrolyte decomposition on the carbon surface should not be ignored because carbons have such a substantially greater surface area than any of the other cell components that the exposed area to electrolyte solution is very large even if the loading of the carbons is not high [13].

The cathodic discharge/charge reactions involved in the present cell system proceed via a dissolution/deposition process. In the discharge reaction, the MnO_2 powders loaded in the composite cathodes are dissolved to produce Mn^{2+} ions whereas as-generated Mn^{2+} ions are re-deposited to MnO_2 during the charging period. Thus, it is very likely that the earlier stage deposition reaction, the nucleation and growth period, takes place on the carbon surface since carbon additive can provide a greater number of deposition sites for Mn^{2+} ions. If this is the case, the nature of loaded carbon additives, particularly their surface states, will control the rate of the charging reaction which will eventually affect the cathodic performance of MnO_2 composite cathodes. With this in mind, we have employed two different types of carbons which differ in the surface polar group population, and have examined the influence of carbons on the reversibility of cathodic cell reactions. In order to gain a greater understanding of the effects of the surface polar group, the carbons have been chemically oxidized further with O_3 and HNO_3 or reduced with H_2. The amount of surface oxygenic groups is assessed utilizing a TPR (temperature-programmed reduction) technique. The carbon-dependent cathodic performance of MnO_2 electrodes is described in the second half of the paper.

2. Experimental

2.1. Materials

Layered-type MnO_2 powders were prepared via thermal decomposition of $KMnO_4$, as described in previous reports [14,15].

The carbon additives used in this work are listed in Table 1. Denka Black (Denki Kagaku Kogyo) and Gulf Acetylene Black (Gulf Oil) belong to acetylene blacks, whereas Ketjen Black ECP600JD (Armak) and Vulcan XC-72 (Cabot) are furnace blacks. The additives were washed with boiling toluene and acetone before use. To control the surface oxygenic group population, Ketjen Black was further treated with 30 wt.% nitric acid at 90°C for 3 h, or contacted with O_3 under a flow rate of 150 cm^3 min^{-1} for 30 min at 20°C. It was also treated with H_2 at 400°C.

To prepare the composite cathodes, MnO_2 powders were mixed with carbon additive and Teflon binder in an appropriate weight ratio. The mixtures were then dispersed in 2-propanol, kneaded and spread on a piece of stainless-steel Exmet (long width dimension = 2 mm; short width dimension = 1 mm; apparent area = 1 cm^2), followed by pressing and drying at 120°C for 30 min. The Zn anodes were prepared similarly with Zn metal powders (Aldrich, 325 mesh), Ketjen Black and Teflon binder (200:2:1 in weight ratio). Both electrodes had the same area of 1×1 cm^2.

Cell performances were tested in a three-electrode cell, in which Zn foil (Aldrich) was used as the reference electrode. In order for the Zn/MnO_2 cells tested in this study to be cathode-limited such that the observed capacities represent those of MnO_2, an excess amount of Zn relative to MnO_2 was loaded in the anodes. Normally, 5–10 mg of MnO_2 powder ($0.9–1.8 \times 10^{-4}$ equiv.) was loaded in the cathodes while 80 mg of Zn powder (2.4×10^{-3} equiv.) was loaded in the anodes. 2 M aqueous $ZnSO_4$ solution, with or without a $MnSO_4$ addition, was used as the electrolyte.

2.2. Instrumentation

Charge/discharge cycling was performed galvanostatically at 0.1–1.2 C rate in the potential range of 1.0–1.9 V

Table 1
Tested carbon blacks and their treatment conditions

Carbon black	Type/treatment conditions	Surface area (m^2 g^{-1})
Denka Black	Acetylene black (Denki Kagaku)/washed with boiling toluene and acetone	61
Gulf Acetylene Black	Acetylene black (Gulf Oil)/washed with boiling toluene and acetone	67
Vulcan XC-72	Furnace black (Cabot)/washed with boiling toluene and acetone	180
Ketjen Black	Furnace black (Armak)/washed with boiling toluene and acetone	1270
Ketjen Black–HNO_3	Treated with 30 wt.% HNO_3 at 90°C for 3 h	1060
Ketjen Black–O_3	Treated with O_3 at 150 cm^3 min^{-1} at 20°C for 0.5 h	1270
Ketjen Black–H_2	Treated with 50 vol.% H_2 in N_2 at 400°C for 5 h	1300

(vs. Zn/Zn^{2+}). XRD studies were performed with a Rigaku X-ray diffractometer (Cu K α, $2\theta = 5–65°$, 2 or 4° min^{-1}). The Mn and Zn contents were analyzed with the ICP (inductively-coupled plasma) technique. The TPR measurements were taken under H_2 flow at 0–800°C. The carbon surface area was analyzed by the BET (Brunauer, Emmett, and Teller) technique.

For electrochemical voltage spectroscopy (EVS) studies [16,17], an EG&G PARC M362 potentiostat and a programmable voltage source were combined to control the applied voltage step, and current was continuously monitored until it decayed to a preset threshold value ($I_{threshold} = 13$ μA). The potential was increased stepwise by dV (= 10 mV). An Orion model 170 conductivity meter was used to measure the electrolyte conductivity.

3. Results and discussion

3.1. Performance of Zn/MnO_2 cells in 2 M $ZnSO_4$ electrolyte

Table 2 summarizes the surface area, chemical composition, powder tap density and product yield of the resulting powders which were obtained by pyrolyzing $KMnO_4$ powders at 250–1000°C in air. From the chemical formulae, the theoretical capacities based on two-electron reaction were calculated and are listed in the last column of Table 2. The surface area shows a tendency to decrease from 18 to 2 m^2 g^{-1} with increasing temperature from 250 to 1000°C. The powder density steadily increases with temperature to reach 1.36 g cm^{-3} at 1000°C.

Fig. 1a shows the discharge capacities that were obtained from Zn/2 M $ZnSO_4/MnO_2$ cells in which the 400°C and 800°C samples were loaded in the composite cathodes. The initial capacities are 40–50% of the theoretical values but the capacities decline drastically within a few cycles. The same undesirable results are observed with the other samples. Fig. 1b shows an EVS profile taken with a composite MnO_2 (800°C) cathode. As shown, the discharge reactions take place in two steps at 1.43 and 1.34 V (vs. Zn/Zn^{2+}) but in the reverse scan, the charging reactions barely occur. From this, the immediate capacity losses shown in Fig. 1a have been ascribed to an incomplete charging of the cathode materials.

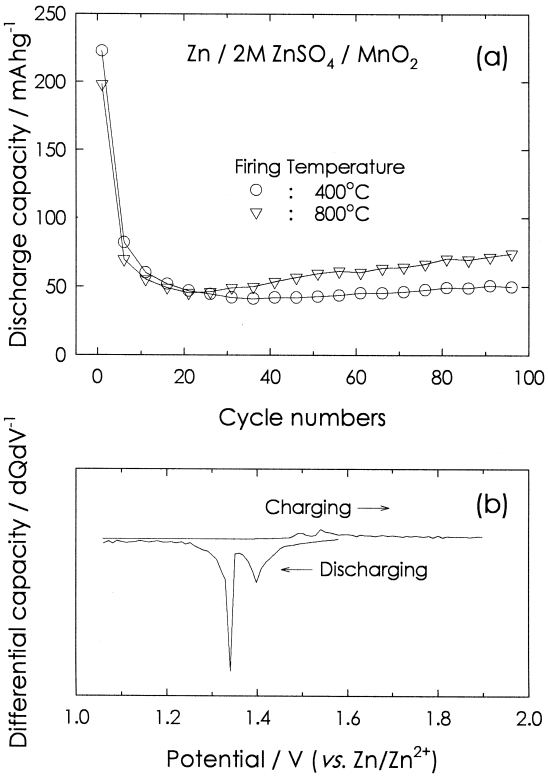

Fig. 1. (a) Discharge capacities of Zn/2 M $ZnSO_4/MnO_2$ cells as a function of cycle number. Charge/discharge cycling was performed galvanostatically at a current density 0.5 mA cm^{-2} (0.1 C) between 1.0–1.9 V (vs. Zn/Zn^{2+}) in 2 M $ZnSO_4$ electrolyte. The composite cathodes consisted of layered MnO_2, Denka Black and Teflon binder (20:10:1 weight ratio). (b) EVS curve recorded with a Zn/2 M $ZnSO_4/MnO_2$ (calcined at 800°C) cell. A 10 mV potential step was imposed and the threshold current was 13 μA. Other experimental conditions were the same as those of (a).

In order to identify further the failure mechanisms associated with the MnO_2 (800°C) cathode, its chemical composition was analyzed with repeated charge/discharge cycling. The Mn and Zn contents in the composite cathode are plotted against cycle number in Fig. 2. As can be seen, during the initial few cycles where a drastic capacity loss is observed, the Zn content increases rapidly while, in turn,

Table 2
Powder properties and theoretical capacities of layered MnO_2 pyrolyzed at different temperatures

Temperature (°C)	Surface area (m^2 g^{-1})	Total Mn content (wt.%)	Mn^{4+} (%)	K^+ (wt.%)	Formula	Powder density (g cm^{-3})[a]	Yield (Mn %)	Capacity (mA h g^{-1})[b]
250	18.4	48.8	96.4	9.30	$K_{0.27}MnO_{2.12} \cdot 0.89H_2O$	0.56	66.6	467
400	16.6	48.5	94.5	10.7	$K_{0.31}MnO_{2.13} \cdot 0.76H_2O$	0.58	72.3	462
600	10.0	49.2	93.9	10.4	$K_{0.30}MnO_{2.12} \cdot 0.61H_2O$	0.75	73.1	466
800	4.9	49.2	91.9	10.4	$K_{0.30}MnO_{2.11} \cdot 0.60H_2O$	1.10	73.3	461
1000	2.3	50.1	85.3	10.6	$K_{0.30}MnO_{2.07} \cdot 0.47H_2O$	1.36	78.6	453

[a] Powder tap density was measured according to ASTM Standard 527-93.
[b] Theoretical capacities based on a two-electron discharge/charge reaction.

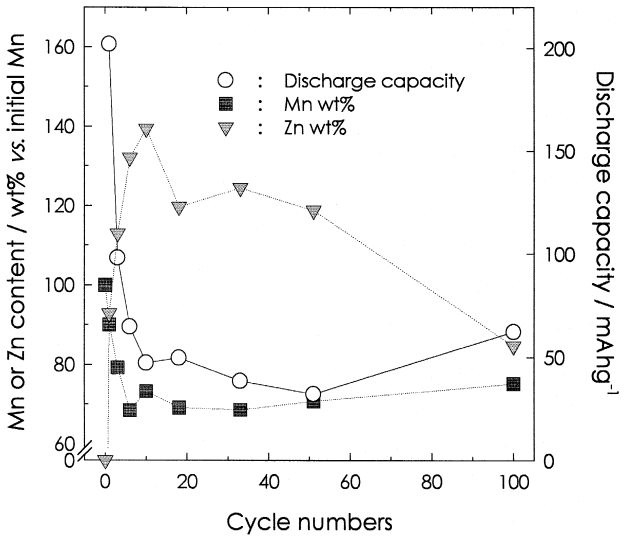

Fig. 2. Variation of discharge capacity of layered MnO_2 (800°C) cathode (right axis) and normalized Mn and Zn contents (left axis) according to cycle number. Cycling conditions were the same as those of Fig. 1a.

the Mn content decreases sharply. The build-up of Zn reaches up to 1.4 times of the initial Mn content, whereas the Mn loss amounts to 30% of the initial value.

Manganese losses from the composite cathodes can be explained in terms of the cell reactions which are involved in MnO_2 electrodes. The discharge reaction proceeds in a two-step, two-electron pathway [18,19], i.e.,

$$MnO_2(s) + H^+ + e^- \rightarrow MnOOH(s) \quad \text{(1st electron discharge)} \qquad (1)$$

$$MnOOH(s) + 3H^+ + e^- \rightarrow Mn^{2+}(aq) + 2H_2O \quad \text{(2nd electron discharge)} \qquad (2)$$

In the first discharge reaction, MnO_2 is transformed to MnOOH which is further reduced to Mn^{2+} at the second step. During the charging period, Mn^{2+} ions are supposed to be oxidized so as to produce a MnO_2 deposit via the MnOOH intermediate. As indicated in Fig. 1b, however, Mn^{2+} ions that are once produced during the discharge period are not fully restored to MnO_2. Thus, it is likely that this incomplete charging leads to a gradual Mn deficiency in the cathode materials, and thereby causes a progressive loss in capacity. With many manganese oxide based cathode materials, Mn dissolution through a disproportionation of Mn^{3+} ions is well documented [20,21]. In this context, a possible Mn dissolution through such a reaction, (a non-faradaic process and thus not related with the discharge reaction) cannot be totally ignored in the present cell system.

The increase in the Zn fraction in the composite cathodes may be due either to Zn^{2+} adsorption on the carbon surface or to the formation of Zn-enriched new phases in the cathodes. The former is not improbable because the carbon additives have a larger surface area than the other cell components, such as the active materials and the current-collectors. The latter possibility is confirmed in this study and also by others [4,22] through an XRD study on once-cycled cathode materials. The XRD patterns taken with a composite MnO_2 cathode are shown in Fig. 3. Initially, only diffraction peaks that belong to the layered MnO_2 appear. But after 10 cycles, new diffraction peaks develop in the pattern. The new phase is identified as the basic zinc sulfate (BZS, $ZnSO_4 \cdot 3Zn(OH)_2 \cdot 4H_2O$) after comparing the diffraction pattern to that of separately synthesized basic zinc sulfate powder.

3.2. Improvement of cell performance with $MnSO_4$ addition

A summary of the results presented so far suggests that the rapid capacity loss is caused by an incomplete charging of the cathodes and the formation of electrochemically inactive BZS on the cathode surface. Therefore, it is very likely that, in order to improve the cathode performance, the cell system should be modified to achieve at least three goals: (i) facilitation of the charging reaction; (ii) suppression of non-faradaic Mn dissolution; (iii) inhibition of BZS formation. In order to accelerate the charging reaction and to discourage Mn dissolution, the addition of Mn^{2+} ions into $ZnSO_4$ electrolyte was conceived to be a reasonable approach. Lowering the solution pH was thought to be a simple way to suppress the formation of BZS because the latter are hardly formed at acidic conditions. The three goals were accomplished in this study by adding small amounts of $MnSO_4$ to the electrolyte. Table 3 lists the pH and conductivity of 2 M $ZnSO_4$ solution as a function of $MnSO_4$ addition. As listed, the $MnSO_4$ addition leads to a decrease in both the solution pH and conductivity. Fig. 4a

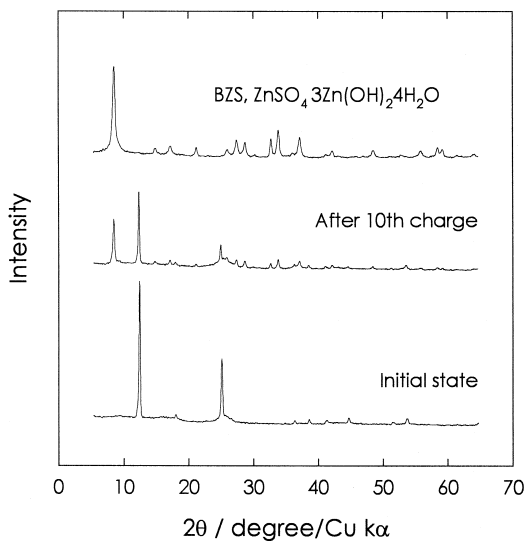

Fig. 3. XRD patterns of separately synthesized BZS powders and composite cathodes in fresh state and after 10 cycles. Cycling conditions were the same as those of Fig. 1a.

Table 3
Solution pH and conductivity of 2 M $ZnSO_4$ electrolytes with addition of $MnSO_4$

Added $MnSO_4$ (M)	pH	Conductivity at 22°C (mS cm^{-1})
0.0	4.32	50.5
0.1	3.06	50.0
0.2	2.74	49.4
0.5	2.31	47.0
1.0	1.94	41.5
2.0	1.48	26.4

shows the discharge capacity profiles of Zn/MnO_2 cells that were obtained in 2 M $ZnSO_4$ electrolytes containing different amounts of $MnSO_4$. Clearly, the addition of $MnSO_4$ improves the initial capacity and also the long-term cyclability. With an increasing addition of $MnSO_4$, the cyclability increases steadily to reach the optimum value at 0.1 M, but it declines thereafter. With 0.1 M $MnSO_4$ addition, the initial capacity increases up to 300 mA h g^{-1} (which amounts to 65% of the theoretical value) and it is retained up to 120 cycles without significant losses. In the meantime, the worse performances with an excessive addition (> 0.5 M) seem to be due to the lower solution conductivity that presumably induces significant cell polarization.

The addition of $MnSO_4$ seems to mitigate the three failure modes. It improves the reversibility of cell reactions by facilitating the charging reaction and discourages both Mn dissolution and BZS formation. An enhancement in reversibility can be noticed in the EVS profile that was obtained in 0.5 M $MnSO_4$ + 2 M $ZnSO_4$ solution (Fig. 4b). In this electrolyte, the charging reaction, which barely occurs without $MnSO_4$ as shown in Fig. 1b, is now greatly facilitated. Two separate peaks corresponding to each charging reaction appear at 1.48 and 1.57 V. Furthermore, the coulombic efficiency (ratio of charging capacity/discharging capacity) approaches unity. Fig. 5a shows the XRD patterns of MnO_2 cathodes which were charge/discharge cycled in different electrolyte solutions. Compared with those cycled in pure $ZnSO_4$ solution, where a significant amount of BZS was deposited, the composite cathodes cycled in the $MnSO_4$ added solutions contain a reduced amount of BZS. The BZS formation is still appreciable at pH 3.06, but becomes negligible at pH 2.31. The

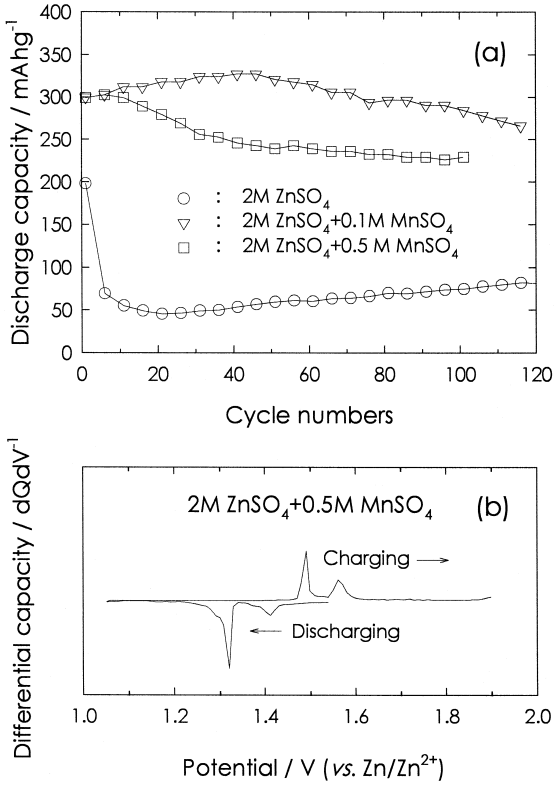

Fig. 4. (a) Discharge capacities of Zn/MnO_2 (800°C) cells according to cycle number. Electrolyte composition is indicated. Charge/discharge cycling was made galvanostatically at a current density of 1 mA cm^{-2} (0.4 C) between 1.0–1.9 V (vs. Zn/Zn^{2+}). Composite cathodes composed of layered MnO_2, Denka Black and Teflon binder (10:20:1 weight ratio). (b) EVS curve of a Zn/MnO_2 cell in 2 M $ZnSO_4$ + 0.5 M $MnSO_4$ electrolyte. Experimental conditions were the same as those of Fig. 1b.

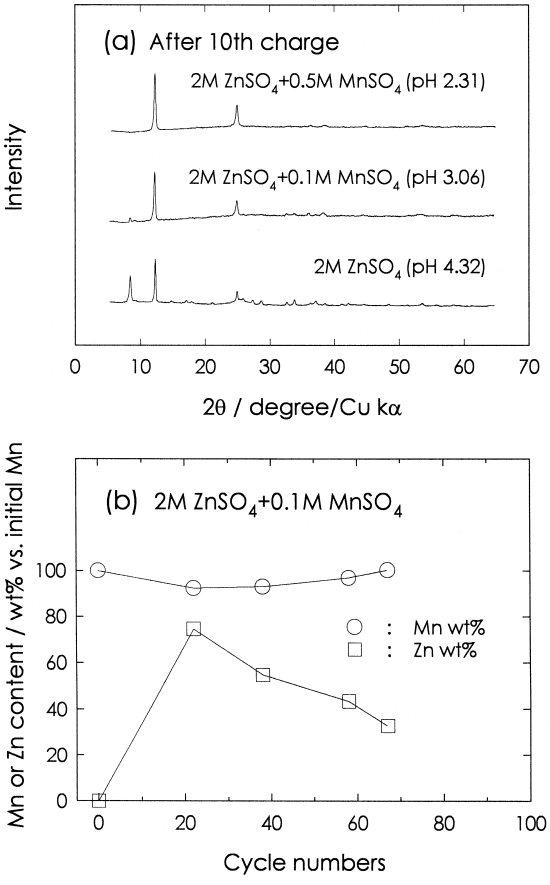

Fig. 5. (a) XRD patterns recorded with composite cathodes after 10 cycles. Electrolyte composition and solution pH is indicated. (b) Normalized Mn and Zn contents in composite cathodes cycled in 2 M $ZnSO_4$ + 0.1 M $MnSO_4$ electrolyte. Cycling conditions were the same as those of Fig. 4a.

chemical composition of cycled MnO_2 cathodes was also analyzed (Fig. 5b). As shown, the Mn contents do not change much. This indicates that the non-faradaic Mn dissolution is not appreciable, and that the cell reactions become very reversible; once-produced, Mn^{2+} ions are largely restored to MnO_2 during the charging period. Nevertheless, the composite cathodes still contain an appreciable amount of Zn, which can be accounted for in terms of BZS formation (Fig. 5a) and Zn^{2+} adsorption on the carbon surface.

3.3. Effects of carbon additives on cathodic charging reactions

It is found that carbon additives loaded in the composite MnO_2 cathodes play an important role in influencing the cathodic performance. For example, as shown in Fig. 6, the initial discharge capacities of MnO_2 cathodes and their long-term cyclabilities are critically dependent on the nature of the employed carbon additives. A general trend is noticed in Fig. 6a, whereby the composite cathodes loaded with furnace blacks exhibit higher initial capacities than

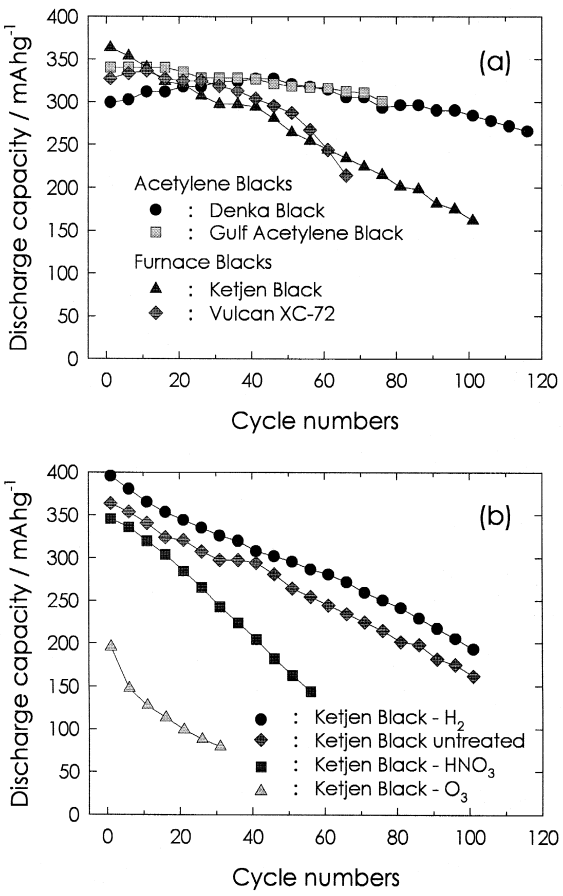

Fig. 6. Discharge capacities of Zn/0.1 M $MnSO_4$ + 2 M $ZnSO_4$|MnO_4 cells according to cycle number. Loaded carbons are indicated. Composite cathodes composed of layered MnO_2 (800°C), carbon additive and Teflon binder (10:20:1 weight ratio). Cycling conditions were the same as those of Fig. 4a.

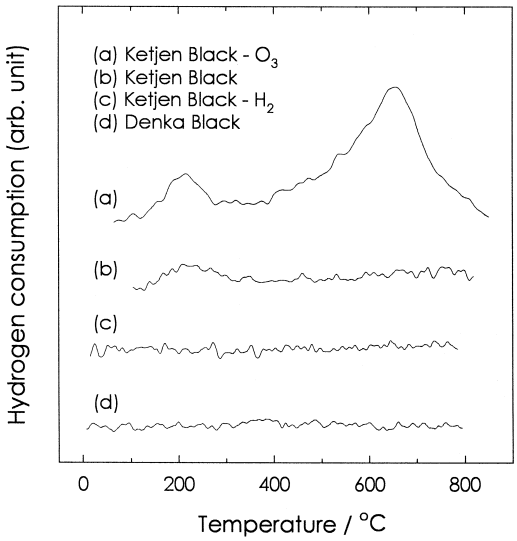

Fig. 7. TPR (temperature-programmed reduction) profiles traced with various carbons. H_2 consumption required to reduce surface oxygenic species is plotted against temperature.

the acetylene black counterparts, but, in turn, their cyclabilities are somewhat poorer. In the case of a Ketjen Black cathode, the initial capacity reaches 370 mA h g^{-1} which amounts to 80% of the theoretical value. The higher initial capacities with furnace blacks are not surprising because their surface area and intrinsic conductivity are both higher than that of acetylene blacks and, consequently, the former cathodes experience less severe cell polarization [12]. [1] The poorer cyclabilities observed with these cathodes cannot, however, be explained in terms of cell polarization. There should be more tenable factors. A clue to this can be found in the results obtained from the chemically treated carbons. As shown in Fig. 6b, the discharge capacities vary significantly according to the surface treatment conditions. For example, when the oxidized carbons are loaded in the MnO_2 cathodes, both the initial capacity and the cyclability are worse than those observed with the untreated carbons. The reverse trend—a larger initial capacity and better cyclability—is noticed with the H_2-treated carbon.

Given the above observation, it is concluded that the cell performance is related closely to the surface states of carbon additives. With this in mind, an analysis was conducted of the surface polar group population on the carbon additives. The TPR (temperature-programmed reduction) results are shown in Fig. 7 in which the H_2 consumption required to reduce surface oxygenic species is plotted against temperature. The H_2 consumption peaks have been assigned on the basis of the results reported by Donnet et al., who performed a similar study on carbons and assigned the 200–300°C peak to the surface carboxylic/lactonic groups and the peak at above 500°C to

[1] Ref. [11], Chap. 2.

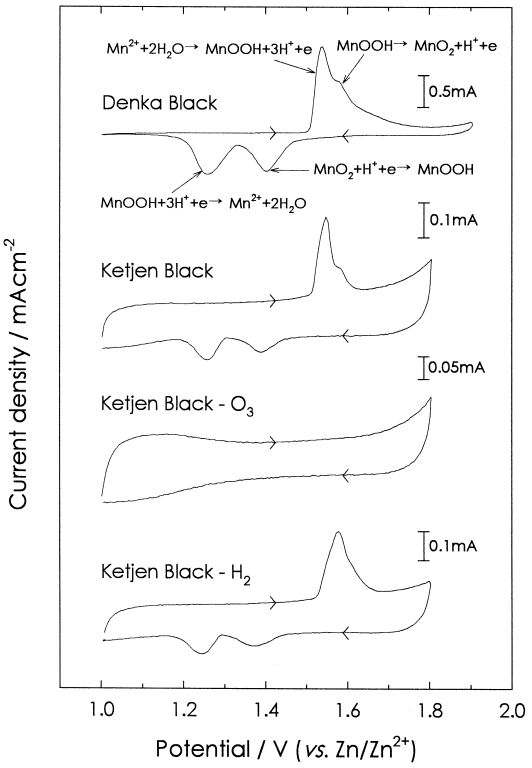

Fig. 8. Cyclic voltammograms comparing the Mn^{2+} oxidation/MnO_2 reduction behaviour on various carbons. Carbon composite electrodes consisted of carbon and Teflon binder (20:1 in weight ratio). Scan rate = 0.1 mV s^{-1}. Note the current scales.

the phenols/quinones. [2] The TPR profile obtained with Denka Black, an acetylene black, indicates that this carbon has a negligible amount of surface oxygenic groups, while Ketjen Black, a furnace black, contains an appreciable amount of carboxylic/lactonic groups. A similar difference is observed between Vulcan XC-72 (furnace black) and Gulf Acetylene Black (acetylene black) whereby the former displays a peak at 200–300°C but the latter does not. This result is in good agreement with the previous results that furnace blacks have a greater number of surface polar groups compared with acetylene blacks [2]. The results in Fig. 7 also indicate that the population of surface oxygenic groups, as expected, increases significantly with chemical oxidation but are diminished after H_2 treatment. Note, the chemical oxidation causes an increase in the population of phenols/quinones so as to give an intense H_2 consumption peak in the range 400–800°C.

A combination of the results shown in Figs. 6 and 7 makes it immediately apparent that the cathode performance of MnO_2 composite electrodes is inversely related to the amount of surface oxygenic groups on the carbon additives. Acetylene blacks, on which the surface oxygenic groups are depleted, give a better cyclability than the surface-group-enriched furnace blacks. Apparently, the poorest cyclability is observed with those containing O_3-treated carbons.

It is now appropriate to explain how the surface oxygenic species on carbons affect the cathodic performance. As described above, the cyclability of MnO_2 cathodes is largely limited by the formation of BZS and also by the sluggish charging reaction. The charging reaction (viz., oxidation of Mn^{2+} ions to MnOOH and further to MnO_2) proceeds via a deposition step such that the highly exposed carbon surface may provide the deposition sites for MnOOH/MnO_2, at least in the earlier stages of nucleation and growth [23–25]. If this is the case, the carbon surface states naturally have a crucial effect on the charging reaction. Accordingly, cyclic voltammograms were recorded to compare the Mn^{2+} oxidation (the charging reaction of the cathode in the present cells) behaviour on various carbon composite electrodes which consist of only carbon additive and Teflon binder (Fig. 8). On the Denka Black (an acetylene black) electrode, Mn^{2+} ions are oxidized in two steps and in the reverse scan, the corresponding reduction peaks appear at two separate potentials. A comparison of the EVS profile in Fig. 4b and the voltammograms in Fig. 8 reveal that the two current peaks in the forward scan correspond to the two-step charging reaction in the present cell system, whereas the reverse peaks are related to the discharge reaction. This observation supports the above premise that the charging reactions in the present cell system take place on the carbon surface. This carbon-dependent feature is more apparent in the other voltammograms in Fig. 8. On the surface-group-enriched Ketjen Black electrode, even if Mn^{2+} oxidation occurs at the identical potential, the oxidation currents and, consequently, the MnO_2 reduction currents are less intense

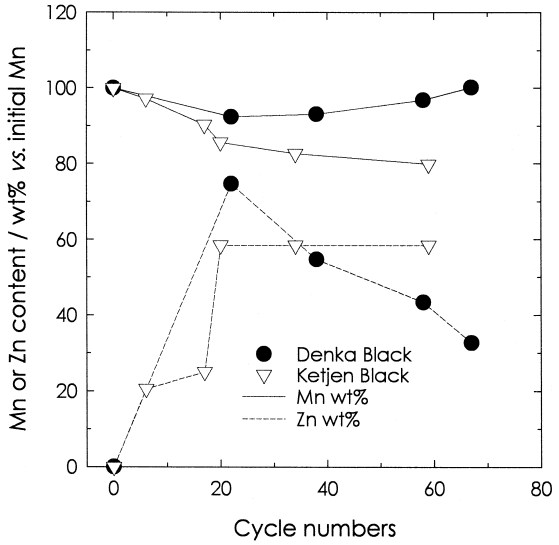

Fig. 9. Variation of Mn and Zn contents in composite MnO_2 cathodes according to cycle number. The composition was normalized against initial Mn contents. Cycling conditions were the same as those of Fig. 4a.

[2] Ref. [12], Chap. 4.

(about one-fifth) than those observed on the Denka Black electrode. Moreover, Mn^{2+} oxidation barely occurs on the ozonized Ketjen Black and, consequently, gives rise to a negligible reduction current.

The chemical composition of cycled MnO_2 composite cathodes was analyzed to compare the reversibility of the cell reactions (Fig. 9). The cells were disassembled after a full charge up to 1.9 V (vs. Zn/Zn^{2+}). The amount (wt.%) of Mn or Zn was normalized against the initial Mn content. As shown, the Mn content does not decrease in the Denka Black loaded cathode even after the cells had been subjected to 70 cycles. This implies that the charge/discharge reaction is so reversible in this cathode that Mn^{2+} ions, once formed by the discharge reaction, are fully reoxidized to MnO_2 during the charging period. In the case of the Ketjen Black cathode, however, 20% of the initial Mn was lost. Thus, the charging reaction in this cathode is much hindered, presumably because high population of surface oxygenic groups prevents the Mn^{2+} ions from being fully reoxidized to MnO_2 during the charging period. On the other hand, both composite cathodes contain appreciable amounts of Zn after cycling. This is due to the formation of BZS or Zn^{2+} adsorption on the carbon surface.

Electron micrographs of the surface region of two MnO_2 composite cathodes in which two different carbons were loaded are presented in Fig. 10. The photographs were taken after the cathodes were charged to 1.9 V in order to observe MnO_2 morphology. The micrograph of the fresh

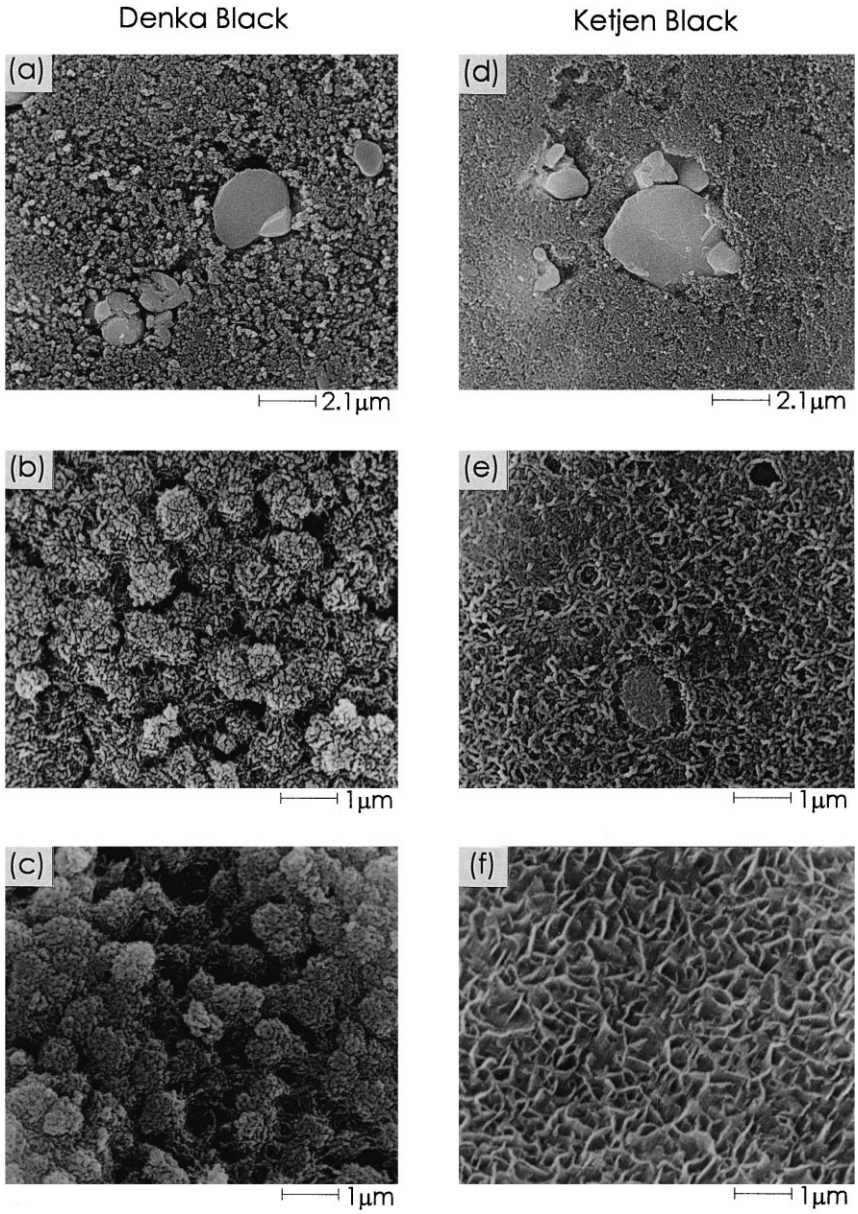

Fig. 10. Electron micrographs of the surface region of composite MnO_2 cathodes. Left panel: Denka Black electrodes; right panel: Ketjen Black electrodes. (a) and (d) before cycling; (b) and (e) after the 5th cycle; (c) and (f) after the 15th cycle. Cycling conditions were the same as those of Fig. 4a.

state (i.e., before cell cycling) indicates that the larger MnO_2 particles are embedded in the carbon/binder matrix (Fig. 10a and d). The two micrographs essentially show the same pattern, except for the size of the carbon particles. When the cells are cycled, however, different morphological transitions develop between the two composite cathodes. With the Denka Black cathode, well-grown granular-shaped MnO_2 deposits appear after the 5th cycle. Even after the repeated dissolution and redeposition process (discharge/charge reaction), the porous and granular shape is maintained throughout the cell life (Fig. 10c). This suggests that the cathodic cell reactions are very reversible. In contrast, on the Ketjen Black cathode, irregular-shaped MnO_2 deposits appear after the 5th cycle (Fig. 10e). After 15 cycles, less porous deposits cover the whole of the electrode surface (Fig. 10f). The MnO_2 grains appear much smaller and the layer is much thinner than that observed in the former electrode. Again, it is concluded that the charging reaction does not readily occur on surface-group-enriched furnace blacks.

4. Conclusions

In this report, we have presented the failure modes of layered MnO_2 cathodes in rechargeable $Zn/ZnSO_4/MnO_2$ cells. Sluggish charging reactions and basic zinc sulfate (BZS) formation are the major degradation mechanisms. In order to improve the cathodic performance, $MnSO_4$ addition to the electrolyte and proper selection of carbon additives are proposed. The following key observations are made.

(1) Layered MnO_2 composite cathodes lose their initial capacity within a few cycles in pure $ZnSO_4$ electrolyte. This drastic decline in capacity is caused by incomplete charging of the cathode materials and by the deposition of basic zinc sulfate on the cathode surface.

(2) Addition of 0.1–0.5 M $MnSO_4$ to 2 M $ZnSO_4$ electrolytes greatly improves the reversibility of the cathodic reactions. In addition, BZS formation is suppressed due to the rather low pH of the $MnSO_4$ added electrolyte.

(3) Cathodes loaded with acetylene black exhibit better cyclability than furnace black cathodes. The differences arise from the extent of charging reactions that is determined by the surface group population on the carbons. Since acetylene blacks possess negligible amounts of surface oxygenic species, Mn^{2+} oxidation (the charging reaction of the cathode in the present cell system) readily occurs on them. By contrast, the charging reaction is sluggish on furnace blacks where the surface oxygenic species are enriched. From this and the further observation that Mn^{2+} oxidation is negligible on the O_3-treated carbons, two conclusions are drawn: (i) the charging (deposition) reaction takes place on the carbon surface, at least in the earlier nucleation and growth period; (ii) the surface oxygenic species control the rate of the charging reaction. MnO_2 deposits are well developed on acetylene blacks and have a porous, granular shape. Moreover, this morphology is maintained throughout cycling and thus demonstrates the very reversible nature of the cathodic reactions on these carbons. On the other hand, the deposition reaction is so sufficiently retarded on the furnace black cathodes that only an irregular-shaped, thin layer of MnO_2 forms on these cathodes.

Acknowledgements

This study was supported by the Korean Ministry of Education through Research Fund.

References

[1] D. Linden (Ed.), Handbook of Batteries, 2nd edn., McGraw-Hill, 1994, Chaps. 8, 10.
[2] C.D.S. Tuck (Ed.), Modern Battery Technology, Ellis Horwood, Chichester, 1991, Chap. 3.
[3] K. Kordesch, M. Weissenbacher, J. Power Sources 51 (1994) 61.
[4] T. Shoji, T. Yamamoto, J. Electroanal. Chem. 362 (1993) 153.
[5] T. Shoji, M. Hishinuma, T. Yamamoto, J. Appl. Electrochem. 18 (1988) 521.
[6] M.H. Askar, H. Abbas, S.E. Afifi, J. Power Sources 48 (1994) 303.
[7] Y.F. Yao, N. Gupta, H.S. Wroblowa, J. Electroanal. Chem. 223 (1987) 107.
[8] L. Bai, D.Y. Qu, B.E. Conway, Y.H. Zhou, G. Chowdhury, W.A. Adams, J. Electrochem. Soc. 140 (1993) 884.
[9] S. Bach, J.-P. Pereira-Ramos, N. Baffier, R. Messina, Electrochim. Acta 36 (1991) 1595.
[10] S. Bach, J.-P. Pereira-Ramos, C. Cachet, M. Bode, L.T. Yu, Electrochim. Acta 40 (1995) 785.
[11] K. Kinoshita, Carbon, Electrochemical and Physicochemical Properties, Wiley, Chichester, 1988, Chap. 7.
[12] J.-B. Donnet, R.C. Bansal, M.-J. Wang (Eds.), Carbon Black, Science and Technology, 2nd edn., Marcel Dekker, New York, 1993, Chap. 8.
[13] D.H. Jang, Y.J. Shin, S.M. Oh, J. Electrochem. Soc. 143 (1996) 2204.
[14] S.H. Kim, S.M. Oh, J. Mater. Sci., submitted.
[15] F.H. Herbstein, G. Ron, A. Weissman, J. Chem. Soc. A (1971) 1821.
[16] J. Barker, Electrochim. Acta 40 (1995) 1603.
[17] J. Barker, R. Koksbang, Solid State Ionics 78 (1995) 161.
[18] A. Kozawa, R.A. Powers, J. Electrochem. Soc. 113 (1966) 870.
[19] A. Kozawa, J.F. Yeager, J. Electrochem. Soc. 115 (1968) 1003.
[20] M.M. Thackeray, R.J. Gummow, A. de Kock, A.P. de la Harpe, D.C. Liles, M.H. Rossouw, Proceedings of 11th Seminar on Primary and Secondary Battery Technology and Application, FL, USA, Feb. 1994.
[21] R.J. Gummow, A. de Kock, M.M. Thackeray, Solid State Ionics 69 (1994) 59.
[22] I. Joy Bear, I.E. Grey, I.E. Newnham, L.J. Rogers, Aust. J. Chem. 40 (1987) 539.
[23] E. Preisler, J. Appl. Electrochem. 19 (1989) 559.
[24] W.-H. Kao, V.J. Weibel, J. Appl. Electrochem. 22 (1992) 21.
[25] H. Zhang, S.-M. Park, J. Electrochem. Soc. 141 (1994) 2422.